

Supplemental Material for “The Frequency Response of Temperature and Precipitation in a Climate Model”

The following figures provide additional information that may be useful in interpreting some results in the paper.

The magnitude of the frequency response for several variables is given in the paper (Fig. 1), Fig. S1 gives the corresponding phase. Because the system is stable and minimum-phase, the phase is directly related to the magnitude of the response. The phase appears to be noisier than the magnitude because there is only a small range of phase across the wide range of forcing frequencies. The diffusion model also gives the best fit to the phase of the response.

The spatial behavior of temperature is given in the paper; the corresponding spatial behavior for precipitation is shown in Fig. S2. There is less of a significant difference in the spatial response pattern of precipitation between the short and long period than there is for temperature.

Fig. S3 maps τ and β from the fit at each grid-point to

$$H_4(s) = \frac{1/\lambda}{1 + (\tau s)^\beta} \quad (\text{S1})$$

(Eq (8) in the paper). As noted, some regions have slope β significantly different from the value of $1/2$ corresponding to diffusion. While the time-scale of the average response is 20 yrs, the time-scale is higher over ocean than land, and can be significantly higher in regions where the surface ocean communicates with the deep ocean. Note that 1.56τ is the time to reach $1/e$ of the final value only for $\beta = 0.5$.

Fig. S4 compares the model frequency response with an empirical transfer function estimate (ETF) based on observational data. The model response is normalized by the approximate radiative forcing, 0.7 times the top-of-atmosphere forcing. The ETF uses the global mean temperature from 1880–2010 and the (highly uncertain) estimated radiative forcing. The time series are divided into 7 overlapping 32-year segments, and Fourier transforms computed for each segment. Auto- and cross-correlations between input (radiative forcing) and output (global mean temperature) are obtained by averaging over the segments; this reduces the contribution due to output that is not correlated with the input. Small changes in the choice of windowing or number of segments can affect the results at periods less than 4 years, and there is insufficient data to reliably estimate the transfer function at periods longer than 32 years. The plotted error bars are based only on the estimated coherence (the fraction of the output variance correlated with the input), and do not take into account the significant uncertainty in the radiative forcing; for this reason, validation of the frequency response based on observed data is challenging.

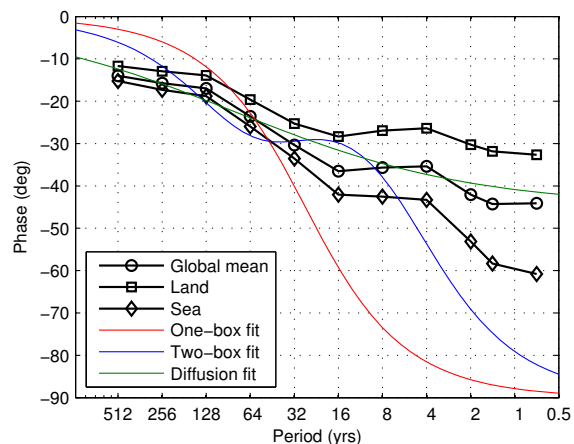


Figure S1. Phase of the temperature relative to the solar forcing as a function of forcing frequency (corresponding to the magnitude of the frequency response in Fig. 1 of the paper). The best-fit of the global mean temperature to the one-box (red) and two-box (blue) energy balance models, and to the diffusion-model (green) are shown. The phase of the land-average and ocean-average response is smaller and larger, respectively, than that of the global mean, consistent with the different slopes of the frequency response magnitude.

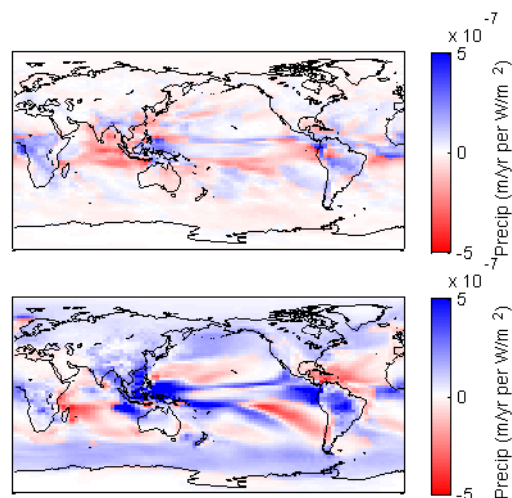


Figure S2. Spatial pattern of precipitation response at a forcing period of $2^{-1/2}$ (top) and 512 years (bottom). The sign of the response is taken as positive (increased precipitation for increased insolation) if the phase between them is between -30 and $+150$ degrees. This binary representation of phase is meaningful at long period, but less so at short period, so sign differences between the plots should not be overinterpreted.

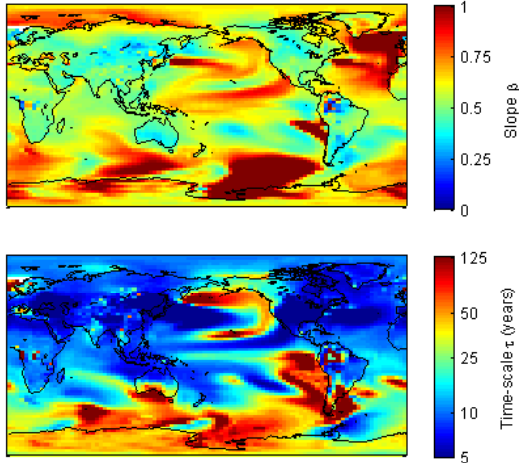


Figure S3. Spatial dependence of best fit of the surface temperature response to the functional form $k/(1 + (\tau f)^\beta)$: slope β (top), and time-scale τ (bottom). The decrease in response with increasing frequency tends to be shallower over continental regions.

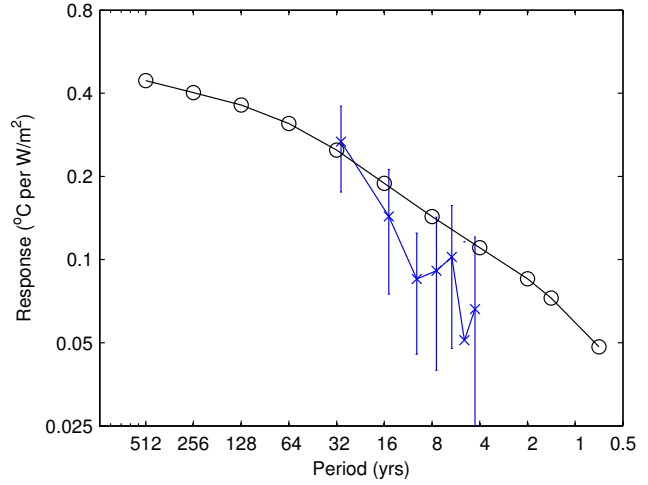


Figure S4. Global mean temperature response to solar radiative forcing at different periods $1/f$ (black, circles), and comparison with an estimate of actual climate response (blue, 'x'). The latter is an empirical transfer function estimate using 1880–2010 observed temperatures and NASA GISS estimated radiative forcing, with ± 1 standard deviation error bars based only on uncorrelated temperature variability, not uncertainty in forcing.